K-P-Means: A Clustering Algorithm of K "Purified" Means for Hyperspectral Endmember Estimation

Linlin Xu, *Student Member, IEEE*, Jonathan Li, *Senior Member, IEEE*, Alexander Wong, *Member, IEEE*, and Junhuan Peng

Abstract—This letter presents K-P-Means, a novel approach for hyperspectral endmember estimation. Spectral unmixing is formulated as a clustering problem, with the goal of K-P-Means to obtain a set of "purified" hyperspectral pixels to estimate endmembers. The K-P-Means algorithm alternates iteratively between two main steps (abundance estimation and endmember update) until convergence to yield final endmember estimates. Experiments using both simulated and real hyperspectral images show that the proposed K-P-Means method provides strong endmember and abundance estimation results compared with existing approaches.

Index Terms—Clustering, endmember estimation, K-P-Means, purified hyperspectral pixel, spectral unmixing.

I. Introduction

ACCURATE estimation of the spectra of pure materials called endmembers is essential to spectral unmixing that aims at estimating for each pixel the fractional abundances of endmembers. Current methods for endmember estimation can be categorized as geometric, statistical, and sparse coding approaches [1]. Although all these approaches have their own respective advantages, it is undeniable that endmember extraction would be more straightforward if we have "pure" pixels that are due to individual endmembers, rather than multiple endmembers, for a number of reasons. First of all, classical geometric approaches that rely on the presence of pure pixels, such as vertex component analysis (VCA) [2], would achieve optimal performance. More intuitively, if we know the group of pixels that are due to a particular endmember, we can just use the mean value of pixels as an estimate of the endmember.

Nevertheless, pure pixels are rare to obtain directly from the hyperspectral images due to factors such as low spatial resolution or the complexity of ground targets.

Given these considerations, this letter therefore intends to explore the feasibility of obtaining "purified" pixels from mixed pixels in order to achieve simplified yet efficient endmember estimation. A "purified" pixel is defined as the residual of mixed pixel after removing the contribution of all endmembers, except the one that dominates the pixel. We estimate "purified" pixels in two steps based on the abundance information of the hyperspectral image. First, we partition all pixels into several groups that are dominated by different endmembers. Second, for pixels in each group, we remove the contributions due to nondominant endmembers in that group. In the first step, since a cluster is defined by predominant endmember, our approach differs from other label-utilizing approaches [3]–[5] in spectral unmixing literature where a cluster may involve multiple significant endmembers. We treat the purified pixels in each group as realizations of endmember subject to random noise and thereby use the expected value of the pixels as the endmember estimate. The resulting algorithm, which we will refer to as a K-P-Means algorithm, alternates iteratively between two main steps (abundance estimation and endmember update) until convergence to yield final endmember estimates. The capability of K-P-Means is proved by experiments on both simulated and real hyperspectral images.

II. Proposed Approach

A. Problem Formulation and Motivation

This letter addresses a linear spectral unmixing model where the observed spectral pixels stack $\mathbf{X}$ is represented by endmember matrix $\mathbf{A}$ and abundance matrix $\mathbf{S}$ with independent and identically distributed (i.i.d.) Gaussian noise $\mathbf{N}$, i.e.,

$$\mathbf{X} = \mathbf{S}\mathbf{A}^T + \mathbf{N} \tag{1}$$

$$\begin{pmatrix} \boldsymbol{x}_1^T \\ \boldsymbol{x}_2^T \\ \vdots \\ \boldsymbol{x}_n^T \end{pmatrix} = \begin{pmatrix} \boldsymbol{s}_1^T \\ \boldsymbol{s}_2^T \\ \vdots \\ \boldsymbol{s}_n^T \end{pmatrix} (\boldsymbol{a}_1, \boldsymbol{a}_2, \dots, \boldsymbol{a}_K)^T + \begin{pmatrix} \boldsymbol{n}^T \\ \boldsymbol{n}^T \\ \vdots \\ \boldsymbol{n}^T \end{pmatrix} \tag{2}$$

where $\boldsymbol{s}_i$ is a $K \times 1$ nonnegative abundance vector that measures the contribution of endmembers $\boldsymbol{a}_j$ $(j = 1, 2, \dots, K)$ to $p \times 1$ dimensional hyperspectral pixel $\boldsymbol{x}_i$, i.e.,

$$\boldsymbol{x}_i = \sum_{j=1}^{K} s_{ij} \boldsymbol{a}_j + \boldsymbol{n}. \tag{3}$$

In most cases, the endmember collection $\{a_j\}$ contribute unequally to x_i, and the group of pixels dominated by a_j is denoted by G_j. Therefore, the image can be partitioned into K sets G_j $(j = 1, 2, \ldots, K)$. In order to reduce the coupling effect among endmembers, it is reasonable to infer a_j $(j = 1, 2, \ldots, K)$ separately from pixels in G_j. Nevertheless, mixed pixels in the same class may still admit multiple endmembers. In order to further remove the influence of less dominant endmembers, it is desirable to use the proportion of x_i that is solely due to the contribution of dominant endmember a_j to estimate a_j, as opposed to using x_i wholly. We refer to x_i after removing the contribution of less dominant endmembers as "purified" pixels.

Not only good abundance information can be utilized to obtain "purified" pixels for enhanced endmember estimation, but accurate endmember estimates can, in turn, boost the accuracy of abundance estimation. Consequently, spectral unmixing can be treated as an iterative optimization issue by taking advantage of the label information from the abundance. We therefore present in the following sections a K-P-Means clustering algorithm that intends to enhance endmember estimation based on the "purified" pixels by explicitly utilizing the label information.

B. K-P-Means Model

This section formulates K-P-Means from a comparative perspective with the classical K-Means algorithm. In K-Means, the spectral vector in class k can be expressed as

$$x_i^k = m^k + n \qquad (4)$$

where m^k is the mean vector of class k, and n is class-independent white noise. Based on the following objective function

$$\{m^k, l\} = \min_{l, m} \sum_{k=1}^{K} \sum_{l_i = k} \|x_i - m^k\|_2 \qquad (5)$$

where $l = \{l_i | i = 1, 2, \ldots, n\}$ are the labels of pixels, K-Means algorithm iterates two steps: estimating l given $\{m^k\}$ and estimating $\{m^k\}$ based on l.

Similarly, the generative model of K-P-Means is formulated as

$$x_i^k = \sum_{j=1}^{K} s_{ij} a_j + n, \qquad \text{where } s_{ik} > \{s_{ij \neq k}\} \geq 0 \qquad (6)$$

where the general term m^k in K-Means is expressed more specifically by $\sum_{j=1}^{K} s_{ij} a_j$. It means that K-Means characterizes a class by the mean vector m^k, whereas K-P-Means defines the class by the dominant endmember a_k, whose abundance s_{ik} is the biggest. Therefore, comparing with K-Means that considers the overall effect of a physical process, K-P-Means probes into the sources of the physical process that contribute to the observations. The object function of K-P-Means can be expressed as

$$\{a_k, l\} = \min_{l, a} \sum_{k=1}^{K} \sum_{l_i = k} \|y_i - a_k\|_2 \qquad (7)$$

where x_i in the objective function of K-Means is substituted by

$$y_i = \left(x_i - \sum_{j \neq k}^{K} s_{ij} a_j \right) \Big/ s_{ik}. \qquad (8)$$

Therefore, as opposed to K-Means that adopts mixed pixels $\{x_i^k\}$ in class k for estimating the mean vector m^k, K-P-Means excludes the contribution of less significant endmembers from estimating dominant endmember a_k. Accordingly, a_k in the proposed algorithm can be treated as the mean vector of "purified" hyperspectral pixels $\{y_i^k\}$. That is why our algorithm is termed K-P-Means. Based on the previously described model, K-P-Means iterates abundance estimation and endmember estimation, just as the two steps in K-Means, which are introduced in Section II-C and D, respectively.

C. Abundance Estimation

Following (7), given $\{a_j\}$, pixel labeling requires solving the following optimization issue:

$$l_i = \arg \min_{k} \left\| \left(x_i - \sum_{j \neq k}^{K} s_{ij} a_j \right) \Big/ s_{ik} - a_k \right\|_2$$
$$\text{s.t.} \quad \{s_{ij}\} \geq 0 \quad \text{and} \quad s_{ik} > \{s_{ij \neq k}\}. \qquad (9)$$

It means that x_i is associated with the kth endmember a_k, which will take the largest coefficient s_{ik} when the representation error is minimized. Suppose $\{a_k\}$ are of similar scale, this optimization issue is equivalent to first estimating $\{s_{ij}\}$ by solving

$$\arg \min_{\{s_{ij}\}} \left\| x_i - \sum_{j}^{K} s_{ij} a_j \right\|_2 \quad \text{s.t.} \quad \{s_{ij}\} \geq 0 \qquad (10)$$

then determining l_i by

$$l_i = \arg \max_{k} \{s_{ik}\}. \qquad (11)$$

As we can see, the estimation of abundance in (10) is essentially a nonnegative least square (NNLS) issue that can be efficiently solved by the method in [8]. Note that the sum-to-one constraint is not necessary since we only need the relative magnitudes of abundances to determine the dominant endmember. Therefore, both K-Means and K-P-Means measure the "relevance" of a pixel to different clusters in order to determine its label. Nevertheless, for K-Means, the "relevance" is measured by the geometric "closeness" from the pixel to class centers, whereas for K-P-Means, it is measured by the magnitude of the nonnegative contribution of endmembers to the representation of the pixel in a least squares sense.

D. Endmember Estimation

Following (7), given $\{y_i^k\}$, K-P-Means updates a^k based on the following generative model:

$$y_i^k = a_k + n. \tag{12}$$

Since n is i.i.d. zero-mean Gaussian noise, the maximum-likelihood estimation of a_k is the expected value of $\{y_i^k\}$. Note that it is possible to apply other endmember extraction techniques, such as VCA on y_i^k, to produce candidates of a_k; it, however, will introduce extra problems, such as the difficulty to determine the most relevant one.

E. Complete Algorithm

Assembling abundance estimation in Section II-C and endmember update in Section II-D into the iterative optimization framework leads to the complete algorithm of K-P-Means, which is detailed in Algorithm 1. In the endmember update step, in order to speed up convergence, the update of an endmember is allowed to utilize the endmembers that have been updated. The iteration of the two steps will stop if either the spectral angle difference (SAD) (see Section III) between endmember estimates in two continuous iterations is smaller than a given value (i.e., τ) or a predefined maximum number of iteration (i.e., $iters$) is reached.

Algorithm 1: K-P-Means

Input: spectral stack $\mathbf{X}$, number of clusters K, and iteration threshold τ;
  Output: endmember $\widehat{\mathbf{A}}$ and abundance $\widehat{\mathbf{S}}$;
  Initialization: $t := 1$, $\widehat{\mathbf{A}}^{(0)} = \text{VCA}(\mathbf{X})$; or
                          $\widehat{\mathbf{A}}^{(0)} =$ randomly selected pixels $\{x_r\}$
  while $t \leq iters$ or $\text{SAD}(\widehat{\mathbf{A}}^{(t)}, \widehat{\mathbf{A}}^{(t-1)}) \geq \tau$ **do**
  (1) $\widehat{\mathbf{S}} = \text{NNLS}(\widehat{\mathbf{A}}^{(t)}, \mathbf{X})$, $\hat{l} \leftarrow \max(\widehat{\mathbf{S}})$;
  (2) **for** $k = 1, 2, \ldots, K$
      $y_i^k = (x_i^k - \sum_{j \neq k}^{K} s_{ij} \widehat{a}_j^{(t)})/s_{ik}$
      $\widehat{a}_k^{(t)} = \text{mean}(\{y_i^k\})$
  end for
  end while

III. EXPERIMENTS

A. Simulated Study

A 64×64 sized image with mixed pixels of four endmembers randomly selected from the U.S. Geological Survey Digital Spectral Library [6] are simulated following the procedure reported in [7]. Using the four endmembers, mixed pixels are created by first dividing the entire image into 8×8 sized homogeneous blocks of one of the four endmembers and then degrading the blocks by applying a spatial low-pass filter of 7×7. To further increase the mixing degree, the remaining relatively "pure" pixels with 80% or larger single abundance are forced to take equal abundances on all endmembers. Zero-mean i.i.d. Gaussian noise is added to further degrade the

image. The resulting image therefore resembles a highly mixed hyperspectral image with measurement errors or sensor noise, which is very challenging for spectral unmixing algorithms.

Two techniques, namely, VCA [2] and minimum volume constrained nonnegative matrix factorization (MVC-NMF) [7], are implemented using the code provided by their authors. VCA represents classical techniques that rely on the existence of pure pixels. Since VCA only extract endmembers, we estimate abundance using NNLS [8]. The comparison with MVC-NMF is desirable since both K-P-Means and MVC-NMF deal with highly mixed pixels. MVC-NMF used as initial parameters the endmember estimated by VCA and 150 iterations in maximum.

Moreover, three variants of K-P-Means are implemented. K-P-Means used as initial parameters both endmembers produced by VCA and raw pixels randomly selected from the data set in order to explore the sensitivity of K-P-Means to initial parameters. The resulting algorithms are referred to as K-P-Means-VCA and K-P-Means-Random, respectively. In K-P-Means-Random, five replicates are performed, each with a new set of initial endmembers, to obtain the solution with the smallest residual. In order to prove the effectiveness of using "purified" pixels in K-P-Means, we introduce for comparison the "nonpurified" approach (i.e., K-nonP-Means), where x_i^k instead of y_i^k is used in Section II-D to update endmembers. All variants are implemented with $iters = 50$ and $\tau = 0.01$ without explicit explanation.

The consistency between estimated endmember $\widehat{a}$ and true endmember a is measured by the widely used spectral angle distance (SAD), defined as $\text{SAD} = \cos^{-1}((a^T \widehat{a})/(\|\widehat{a}\|\|a\|))$, and the spectral information divergence (SID), expressed as $\text{SID} = D(a/\widehat{a}) + D(\widehat{a}/a)$, where $D(x/y)$ measures the relative entropy between x and y [9]. The numerical measures for abundance s are achieved by replacing a with s in SAD and SID. The resulting measures are called AAD and AID, respectively.

The five methods are performed on simulated image to produce numerical measures. In order to investigate the noise robustness of different methods, they are tested on images with different noise levels measured by the signal-to-noise ratio (SNR) [7]. For each noise level, 20 images with independent noise realizations are processed to obtain statistics of numerical measures, as reported in Fig. 1.

Overall, K-P-Means-VCA achieved much smaller mean SAD and SID values than VCA and close results to MVC-NMF across all noise levels, indicating that K-P-Means is capable of extracting accurately the endmembers in highly mixed and noisy circumstance. Moreover, the endmember estimation of K-P-Means-VCA measured by SAD and SID seemed to be robust to the noise level. As we can see, SAD and SID remained at very low values with SNR decreasing from 45 to 20, although from 20 to 10, there was a large increase in SAD and SID. When SNR = 10, we noticed that K-P-Means-VCA achieved smaller SAD and SID than MVC-NMF.

In terms of abundance estimation, K-P-Means-VCA outperformed VCA according to the mean AAD and AID values across all noise levels. The variances of AAD and AID are also smaller in K-P-Means-VCA than in VCA. MVC-NMF achieved lower AAD and AID values than K-P-Means-VCA.
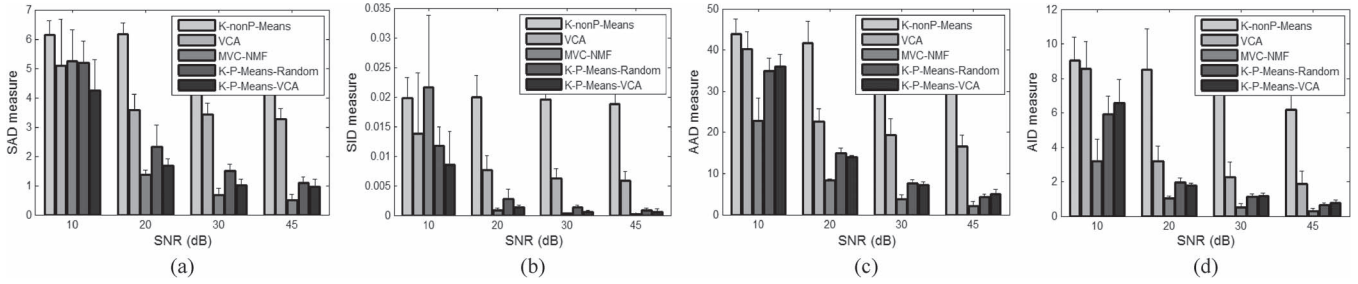
Fig. 1. Performance comparison at different noise levels in terms of (a) SAD, (b) SID, (c) AAD, and (d) AID. In these four statistics, smaller value means better result.

TABLE I
PERFORMANCE OF K-P-MEANS-VCA AND VCA, MEASURED BY MEAN SID AND AID, OVER DIFFERENT IMAGE
SIZES AND VARYING NUMBERS OF ENDMEMBERS

		Image size				Number of endmembers				
		64	128	256	512	4	6	8	12	15
SID*1000	K-P-Means	1	0.5	0.3	0.6	1	2	14	21	50
	VCA	7.5	5.1	5.6	5.6	6	10	59	57	100
AID	K-P-Means	1.0	0.9	0.8	1.0	0.9	2.0	3.4	6.1	6.9
	VCA	2.6	1.5	1.5	1.7	1.8	4.9	6.8	8.9	12.9

However, this advantage is less significant at the low noise level. Overall, these results demonstrate that K-P-Means-VCA can achieve fairly accurate abundance estimation, although it is primarily designed for enhanced endmember extraction.

The observation that K-nonP-Means performed worse than K-P-Means-VCA and K-P-Means-Random demonstrates the importance and benefits of using "purified" pixels instead of the original pixels for endmember estimation. K-P-Means-Random outperformed VCA in terms of all measures across all noise levels, indicating that K-P-Means is capable of achieving acceptable performance with random initializations. It is not surprising that K-P-Means-VCA performed better than K-P-Means-Random, considering the fact that good initial parameters can optimize the convergence properties of ill-posed optimization problems.

Endmember estimation by VCA was insensitive to the noise level change. SAD and SID stayed almost unchanged with SNR decreasing from 45 to 20. MVC-NMF performed better than the rest of the techniques in most cases, although its performance of endmember estimation decreased very fast from SNR = 20 to 10. We noticed that MVC-NMF performed very well when SNR = 10 in [7]. This inconsistency is probably because we used different endmembers for simulation.

In order to explore the sensitivity of K-P-Means to image size and number of endmembers, Table I presents the performances of VCA and K-P-Means-VCA, measured by mean SID and AID, over increasing image sizes from 64×64 to 512×512 and the numbers of endmembers from 4 to 15. Generally speaking, K-P-Means is not sensitive to the increase in image size, and the mean SID and AID values that achieved by K-P-Means-VCA are, respectively, around 10% and 50% of those achieved by VCA. However, the performances of both VCA and K-P-Means-VCA deteriorated with the increase in the number of endmembers. Nevertheless, the SID and AID values achieved by K-P-means are, respectively, 25% and 50% of the statistics achieved by VCA on average.
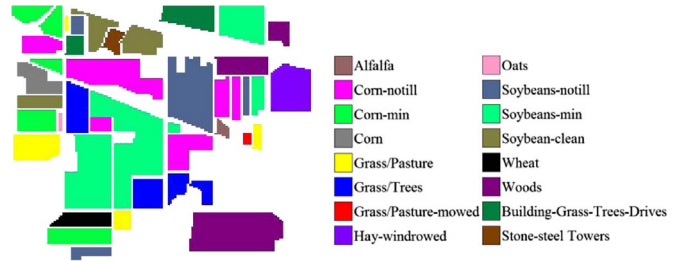

Fig. 2. Ground-truth map of 16 classes in AVIRIS Indian Pines image.

All algorithms were implemented under the MATLAB platform. On average, it took 0.04, 6.51, and 26.24 s, respectively, by VCA, K-P-Means-VCA, and MVC-NMF to process images with 64×64 pixels, on a personal computer with a Pentium 2.30-GHz Quad-Core processor.

B. Test on Real Hyperspectral Images

The Indian Pines image, which was captured by Airborne Visible/Infrared Imaging Spectrometer (AVIRIS) over a vegetation area in northwestern Indiana, USA, is used to test the proposed algorithms. The image has spatial resolution of 20 m and contains 200 spectral reflectance bands after removing 20 water absorption bands (104–108, 150–163, and 220). The image consists of 145×145 pixels belonging to 16 different land cover types, as shown in Fig. 2.

In this experiment, K-P-Means-Random with $iters = 50$ and $\tau = 0.01$ extracted a number of 20 endmembers from pixels covered by ground-truth classes. The abundance maps of eight selected endmembers are shown in Fig. 3(a). As we can see, the maps from left to right, top to bottom correspond, respectively, to Grass/Trees, Hay-windrowed, Grass/Pasture, Soybeans-min, Corn-notill, Wheat, Wood, and Stone-steel Towers. These correspondences between abundance maps and ground-truth classes may indicate that K-P-Means accurately identified the
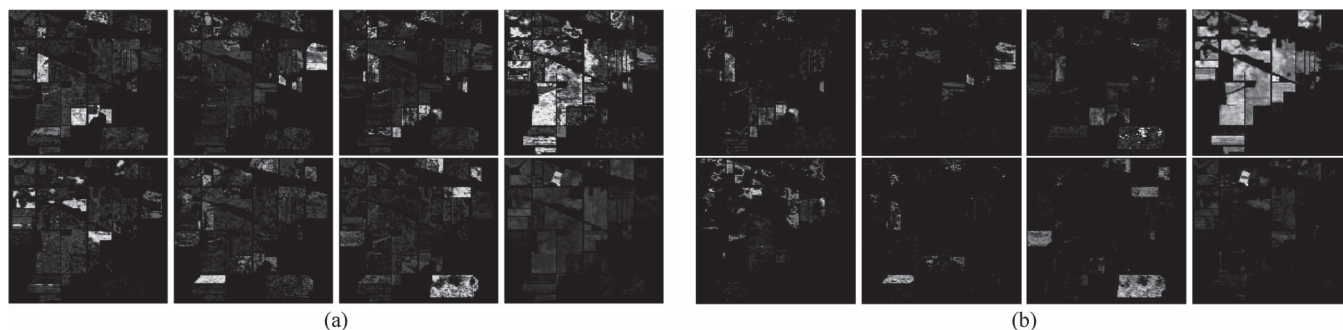
Fig. 3. (a) Abundance maps of eight selected endmembers extracted by K-P-Means-Random. (b) Abundance maps of the corresponding eight endmembers extracted by MVC-NMF.

endmembers in the image, considering that different endmembers tend to dominate different classes. Nevertheless, the bright areas of most abundance maps do not match very well the ground truth, except Wheat and Stone-steel Towers. It is not surprising considering the gap that while K-P-Means is designed to identify individual endmembers, the pixels in the same ground-truth class may actually assume multiple significant endmembers, due to the complexity of ground targets in Indian Pines image.

Fig. 3(b) shows the maps of the eight corresponding endmembers achieved by MVC-NMF for comparison purposes. As we can see, most endmember maps achieved by MVC-NMF do not match the ground truth as well as the maps achieved by K-P-means, except the two maps corresponding to Wheat and Stone-steel Towers.

IV. CONCLUSION

This letter has presented a K-P-Means algorithm for hyperspectral endmember extraction. Based on abundance information, we proposed to obtain the "purified" pixels from the original mixed pixels for enhanced endmember estimation, which can, in turn, aid abundance estimation. Therefore, we interpreted spectral unmixing as an iterative optimization problem and designed the K-P-Means algorithm that alternates iteratively between two main steps (abundance estimation and endmember update) until convergence to yield final endmember estimates. Experiments on both simulated and real hyperspectral images proved that K-P-Means is capable of accurately estimating both endmembers and abundance.

REFERENCES

[1] J. M. Bioucas-Dias, A. Plaza, N. Dobigeon, M. Parente, Q. Du, P. Gader, and J. Chanussot, "Hyperspectral unmixing overview: Geometrical, statistical, and sparse regression-based approaches," *IEEE J. Sel. Topic Appl. Earth Observ. Remote Sens.*, vol. 5, no. 2, pp. 354–379, Apr. 2012.

[2] J. M. P. Nascimento and J. M. Bioucas-Dias, "Vertex component analysis: A fast algorithm to unmix hyperspectral data," *IEEE Trans. Geosci. Remote Sens.*, vol. 43, no. 4, pp. 898–910, Apr. 2005.

[3] A. Castrodad, Z. Xing, J. Greer, E. Bosch, L. Carin, and G. Sapiro, "Learning discriminative sparse representations for modeling, source separation, and mapping of hyperspectral imagery," *IEEE Trans. Geosci. Remote Sens.*, vol. 49, no. 11, pp. 4263–4281, Nov. 2011.

[4] A. Zare and P. Gader, "PCE: Piecewise convex endmember detection," *IEEE Trans. Geosci. Remote Sens.*, vol. 48, no. 6, pp. 2620–2632, Jun. 2010.

[5] G. Martín and A. Plaza, "Region-based spatial preprocessing for endmember extraction and spectral unmixing," *IEEE Geosci. Remote Sens. Lett.*, vol. 8, no. 4, Jul. 2011.

[6] R. N. Clark, G. A. Swayze, A. Gallagher, T. V. King, W. M. Calvin, The U.S. Geological Survey Digital Spectral Library: Version 1: 0.2 to 3.0 μm, Washington, DC, USA, 1993, Open File Rep. 93-592.

[7] L. Miao and H. Qi, "Endmember extraction from highly mixed data using minimum volume constrained nonnegative matrix factorization," *IEEE Trans. Geosci. Remote Sens.*, vol. 45, no. 3, pp. 765–777, Mar. 2007.

[8] C. L. Lawson and R. J. Hanson, *Solving Least Squares Problems*. Englewood Cliffs, NJ, USA: Prentice-Hall, 1974, ch. 23, p. 161.

[9] C.-I. Chang and D. C. Heinz, "Constrained subpixel target detection for remotely sensed imagery," *IEEE Trans. Geosci. Remote Sens.*, vol. 38, no. 3, pp. 1144–1159, May 2000.